

Large In-plane Anisotropy on Resistivity and Thermopower in The Misfit Layered Oxide $\text{Bi}_{2-x}\text{Pb}_x\text{Sr}_2\text{Co}_2\text{O}_y$

Takenori FUJII^{1,2*}, Ichiro TERASAKI^{1,2}, Takao WATANABE³ and Azusa MATSUDA⁴.

¹*Department of Applied Physics,*

Waseda University, Tokyo 169-8555, Japan.

²*Precursory Research for Embryonic Science and Technology,*
Japan Science and Technology Corporation,

Kawaguchi 332-0012, JAPAN.

³*NTT Photonics Laboratories,*

Kanagawa 243-0198, JAPAN.

⁴*NTT Basic Research Laboratories,*

Kanagawa 243-0198, JAPAN.

(Dated: October 29, 2018)

We investigated the in-plane anisotropy on the resistivity and thermopower of $\text{Bi}_{2-x}\text{Pb}_x\text{Sr}_2\text{Co}_2\text{O}_y$ single crystals, which have a misfit structure between the hexagonal CoO_2 layer and the rock salt $\text{Bi}_2\text{Sr}_2\text{O}_4$ layer. The resistivity and thermopower show significantly large anisotropy, which exceeds two at maximum. This anisotropy would come from the anisotropic pseudogap formation enhanced by the misfit structure. The thermopower changes with Pb doping to take a maximum at $x=0.4$. The misfit structure improves the thermoelectric properties through chemical pressure. The power factor is as large as $9 \mu\text{W}/\text{cmK}^2$ at 100 K for $x=0.6$, which is the highest value for thermoelectric oxides at 100 K.

PACS numbers:

The strongly correlated electron systems in oxide often show unusual physical properties, such as high- T_c superconductivity in cuprates and colossal magnetoresistance in manganites. Recently, layered cobalt oxides NaCo_2O_4 [1], Ca-Co-O [2, 3], Bi-Sr-Co-O [4, 5], and Tl-Sr-Co-O [6] were found to show a large thermoelectric power, and exhibited a potential advantage for thermoelectric material. We have previously pointed out that the high thermoelectric performance of the layered cobalt oxides cannot be explained by a conventional band picture, and proposed that the strong electron-electron correlation plays an important role in the large thermoelectric power [7].

The layered cobalt oxides with large thermoelectric power consist of the alternating stack of a conducting CoO_2 layer and an insulating blocking layer. The Bi-Sr-Co-O system was first thought as having a structure isomorphic to that of the superconducting compound $\text{Bi}_2\text{Sr}_2\text{CaCu}_2\text{O}_{8+\delta}$ (Bi-2212). However, it turned out that the square $\text{Bi}_2\text{Sr}_2\text{O}_4$ lattice lies on the triangular CoO_2 lattice with a misfit along the b axis [8]. Similar crystal structure was reported in $(RX)_xMX_2$ ($R = \text{La, Ce, Sm, Gd, Yb}$; $M = \text{Ti, V, Nb}$; $X = \text{S, Se}$), where the square RX layer was intercalated between the triangular MX_2 layers [9]. These intercalated units weakly couple with conductive MX_2 layers via the van der Waals force. In the case of the Bi-Sr-Co-O system, the coupling between the $\text{Bi}_2\text{Sr}_2\text{O}_4$ layer and the CoO_2 layer is ionic and much stronger than these materials. Therefore,

due to the subcells with different symmetries, the symmetry of the electronic states would be altered to induce in-plane anisotropy in physical properties. Moreover the misfit structure would induce chemical pressure along the b -axis direction. We further note that another structural feature in the Bi-Sr-Co-O system is a strongly modulated BiO layer, as is similarly seen in Bi-2212 [10] along the b axis, which disappears with Pb doping [11]. Thus, Bi-Sr-Co-O system is very complicated with the misfit and modulation structures. It is interesting how the electric properties are affected by the misfit and modulation structures. Here, we report on the in-plane anisotropy on the resistivity and thermopower of the Bi-Sr-Co-O system.

Single crystals of $(\text{Bi,Pb})\text{-Sr-Co-O}$ were grown by a traveling solvent floating zone (TSFZ) method. Starting composition was $\text{Bi}_{2-x}\text{Pb}_x\text{Sr}_2\text{Co}_2\text{O}_y$ ($x=0, 0.4, 0.6, 0.8$). The actual composition was analyzed through inductively coupled plasma-atomic emission spectroscopy (ICP) and energy dispersive X-ray analysis (EDX). Structural analysis was performed using four-circle X-ray diffractometer (Cu K_α X-ray source) and transmission electron microscope (TEM). The resistivity was measured using a standard four probe method. The thermopower was measured using a steady-state technique.

The chemical compositions of the samples used for this study are listed against the nominal composition in Table 1(a). Hereafter, we will refer the samples as the nominal composition of Pb ($x=0, 0.4, 0.6, \text{ and } 0.8$). The EDX and ICP data are in excellent agreement with each other, where $(\text{Bi+Pb}) : \text{Sr} : \text{Co} \sim 2.1 : 2.1 : 2.0$. We can see that the actual composition of Pb is roughly equal to the nominal composition except for $x=0.8$. $x=0.6$ and $x=0.8$

*E-mail address: fujii@htsc.phys.waseda.ac.jp

TABLE I: (a) Chemical composition estimated from energy dispersive X-ray (EDX) analysis and inductively coupled plasma-atomic emission spectroscopy (ICP). (b) Lattice parameter determined from four-circle X-ray diffractometer. b_{RS} and b_H are the b -axis length of the rock-salt and the hexagonal subcells, respectively. b_H is determined by the electron diffraction patterns.

(a) Composition					
Sample		Bi	Pb	Sr	Co
$x=0$	EDX	2.21	0	2.20	2.0
	ICP	2.1	0	2.1	2.0
$x=0.4$		1.61	0.40	2.09	2.0
		1.82	0.42	2.18	2.0
$x=0.6$		1.58	0.57	2.13	2.0
		1.60	0.60	2.10	2.0
$x=0.8$		1.60	0.55	2.15	2.0
		-	-	-	-

(b) Lattice parameter					
Sample	a_{RS} (Å)	b_{RS} (Å)	c (Å)	b_H (Å)	β (deg.)
$x=0$	4.937	5.405	29.875	2.8	93.554
$x=0.4$	4.914	5.221	29.974	2.8	92.315
$x=0.6$	4.904	5.206	30.041	-	92.657

exhibit no difference in the actual chemical composition, the lattice constant, and the transport properties, which indicates that the solubility limit of Pb is considered to be about $x=0.6$.

The lattice constants and the angle β are listed in Table 1(b). With increasing Pb concentration, the c -axis length expands continuously from 29.84 Å of $x=0$ to 30.04 Å of $x=0.6$, whereas the b -axis length of the rock-salt layer b_{RS} discontinuously shrinks from 5.38 Å of $x=0$ to 5.22 Å of $x=0.4$ with the a -axis length of the rock-salt layer a_{RS} nearly unchanged (4.9 Å). This is in good agreement with the powder XRD measurement by Yamamoto *et al* [12].

Figures 1(a) and (b) show the TEM diffraction patterns of $x=0$ and 0.4, respectively, which clearly show a rock-salt diffraction pattern from the $\text{Bi}_2\text{Sr}_2\text{O}_4$ layer and a hexagonal diffraction pattern from the CoO_2 layer. The a - and b -axis length of the hexagonal CoO_2 layer (a_H , b_H) is estimated to be about 2.8 Å and the angle between them is about 60° , which is independent of x within the resolution limit of the TEM image. From the above structural analysis, the prepared samples show the misfit structure along the b axis ($13 b_H \sim 7 b_{RS} \sim 36$ Å), while the a -axis length of the rock-salt layer matches with that of the hexagonal layer ($a_{RS} \sim \sqrt{3} a_H \sim 4.9$ Å). The TEM diffraction pattern of $x=0$ shows satellite reflection due to the modulation structure along the oblique direc-

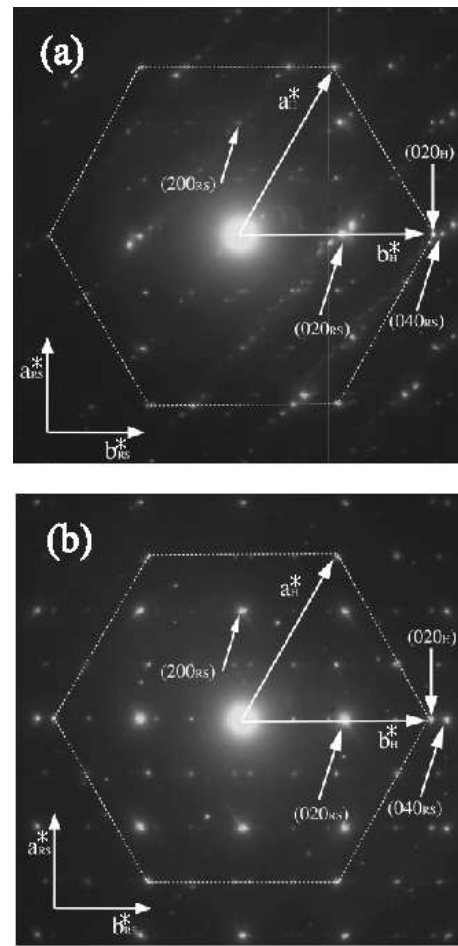


FIG. 1: Electron diffraction patterns of (a) $x=0$ and (b) $x=0.4$.

tion (tilted about 45°) from a_{RS}^* or b_{RS}^* . In contrast, there is no satellite reflection in $x=0.4$, indicating that the modulation structure disappears in this compound. This modulation structure was also confirmed with the Laue transmission photographs (not shown here).

Figure 2 shows the temperature dependence of the a - and b -axis resistivities (We refer the a - and b -axis directions as the a_{RS} and b_{RS} directions). All the samples show a metallic behavior at room temperature. With Pb doping, the magnitude of the resistivity continuously decreases, suggesting that carriers are doped through the substitution of divalent Pb^{2+} for trivalent Bi^{3+} [5, 12]. Note that the magnitude of resistivity for all samples is unusually large for a metal. The large ρ comes from a short in-plane mean free path (~ 3 Å at 300 K) which is comparable to the Co-Co bond length, and suggests the inherent nature of the metallic behavior (These materials are called bad metal) [13].

The in-plane anisotropy of the resistivity (ρ_b/ρ_a) is shown in the inset of Fig. 2. Contrary to the relatively small ρ_b/ρ_a for $x=0$, ρ_b/ρ_a of $x=0.4$ increases strongly below 50 K. This comes from the different temperature dependence; ρ_b shows an upturn below 50 K,

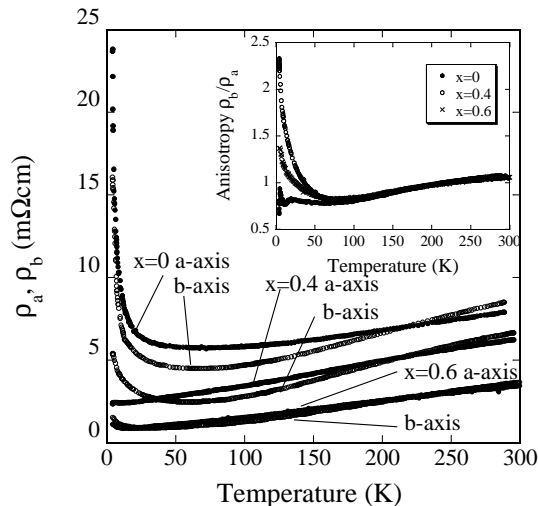


FIG. 2: Temperature dependence of the a - and b -axis resistivities. Inset: In-plane anisotropy of the resistivity (ρ_b/ρ_a).

whereas ρ_a remains metallic down to 4.2 K. Pb substitution for Bi strongly suppresses the low-temperature upturn and $x=0.6$ is again less anisotropic. (Since ρ_a is sensitive to the current direction, a small upturn of ρ_a of $x=0.6$ is possibly due to the misalignment of the contacts.) Since the triangular CoO_2 layer itself shows no in-plane anisotropy, the observed anisotropy is anomalously large from the viewpoint of group theories. This is considered to come from the rock-salt $\text{Bi}_2\text{Sr}_2\text{O}_4$ layers of different symmetry. Actually, Bi-2212, which consists of the square CuO_2 and the rock-salt $\text{Bi}_2\text{Sr}_2\text{O}_4$ layers, shows much less in-plane anisotropy in the resistivity [14]. We have previously proposed the pseudogap formation in Bi-Sr-Co-O at low temperatures [5], and have attributed the upturn of the low temperature resistivity to the decrease in the density of states. Accordingly, the in-plane anisotropy suggests that the pseudogap is anisotropic (nearly zero along the a axis).

Figures 3(a), (b) and (c) show the temperature dependence of the a and b axis thermopower for $x=0$, 0.4 and 0.6 respectively. Pb substitution for Bi enhances the thermopower in both directions from $x=0$ to 0.4. For example, the magnitude of the a -axis thermopower increases from 140 to 160 $\mu\text{V}/\text{K}$ at room temperature in going from $x=0$ to 0.4. However, it decreases down to 140 $\mu\text{V}/\text{K}$ for $x=0.6$. We have claimed that the large thermopower in Co oxides is attributed to the strong electron-electron correlation [5]. The increase of the thermopower from $x=0$ to 0.4 is considered to be due to the discontinuous shrink of the b_{RS} axis, which causes a chemical pressure along the b axis. A similar phenomenon is seen in the Ce-based compounds [7], where the thermopower increases with increasing pressure [15]. The decrease of the thermopower from $x=0.4$ to 0.6 is possibly due to the increase of the carrier density, because the b -axis length is nearly unchanged.

Next, we consider the anisotropy in the thermopower.

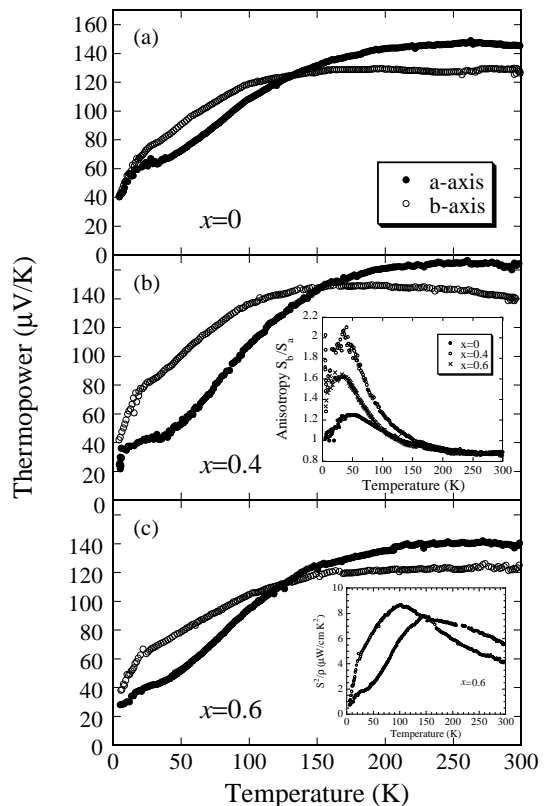


FIG. 3: Temperature dependence of the a - and b -axis thermopower for (a) $x=0$, (b) $x=0.4$, and (c) $x=0.6$. Inset of (b): In-plane anisotropy of the thermopower (S_b/S_a). Inset of (c): The power factor (S^2/ρ) of $x=0.6$ along the a - and b -directions.

In the inset of Fig. 3(b), we show the in-plane anisotropy of the thermopower (S_b/S_a). All the samples exhibit a large anisotropy which is characterized by a larger b -axis thermopower below 100 K. At around 50K, the b -axis thermopower of $x=0.4$ is about two times larger than the a -axis thermopower. Note that the temperature dependence of S_b/S_a roughly corresponds to that of ρ_b/ρ_a . The magnitude of S_b/S_a also agrees with that of ρ_b/ρ_a , where $x=0.4$ shows the largest value of two. These results strongly suggest that S_b/S_a and ρ_b/ρ_a are predominantly determined by the density of states, and that the scattering time is essentially temperature-independent, which is consistent with the bad-metal picture. In this context, S_b/S_a comes from the anisotropic density of states induced by the anisotropic pseudogap. One may notice that the anisotropy of the resistivity is smaller than that of the thermopower for $x=0$. We attribute this to the modulation structure, which works as anisotropic scattering center for Bi-2212 [14].

The power factor (S^2/ρ) is a measure of the thermoelectric properties, which means that large thermopower and low resistivity are required to thermoelectric materials. The power factor along the b axis for $x=0.6$ is more than two times as large as that along a axis at around

50 K (Inset of Fig. 3(c)), which indicates that the thermoelectric properties can be improved (doubled in the present case) with controlling the misfit structure. The magnitude reaches as large as $9 \mu\text{W}/\text{cmK}^2$ that is highest for thermoelectric oxides at 100 K.

Finally, let us discuss the origin of the anisotropic pseudogap. We have previously proposed that a spin-density-wave (SDW)-like state is a possible origin for the pseudogap in NaCo_2O_4 [16]. SDW is closely related to the topology of the Fermi surface and its nesting, and thus the pseudogap is favorable to open along a nesting vector. Assuming that the hexagon-like Fermi surface calculated for NaCo_2O_4 [17] is also applicable for the Bi-Sr-Co-O system, we expect that SDW is formed along the six-fold Γ -K direction. The misfit structure lowers the crystal symmetry of the CoO_2 layer to suppress the nesting along the a -axis direction. Considering that disorder induces an SDW-like transition in NaCo_2O_4 , we think that the misfit structure is likely to enhance the SDW instability in the Bi-Sr-Co-O system.

Another scenario is based on the fact that the in-plane anisotropy of the Bi-Sr-Co-O system is as large as that of $\text{YBa}_2\text{Cu}_3\text{O}_y$ for the heavily oxygenated sample of $y=7$ and the oxygen deficient sample of $y=6.35$ [18]. There are additional conductive CuO chains in $y=7$, which are responsible for the large anisotropy. With decreasing

oxygen content, the CuO chains are progressively destroyed, and the orthorhombicity almost vanishes in $y=6.35$. The large anisotropy in $y=6.35$ is attributed to a self-organization of the two-dimensional electrons, such as a charge stripe. In this sense, there is a possibility that the in-plane anisotropy in the Bi-Sr-Co-O system comes from a charge stripe.

In conclusion, we grew single crystals of $\text{Bi}_{2-x}\text{Pb}_x\text{Sr}_2\text{Co}_2\text{O}_y$ by a TSFZ method. From the structural analysis, we confirmed that they have a misfit structure along the b axis, and that $x=0$ exhibits a modulation structure, whose direction is tilted by about 45° from the a - and b -axes. We found that the resistivity and thermopower shows a large anisotropy, which would come from the anisotropic pseudogap formation. Accordingly the pseudogap in the b_{RS} -axis direction makes the resistivity nonmetallic, and the thermopower larger at low temperatures. Aside from the pseudogap, the misfit structure enhances the thermopower through chemical pressure, and we suggest that we can improve the thermoelectric properties by controlling the misfit structure. The maximum power factor is as large as $9 \mu\text{W}/\text{cmK}^2$ at 100 K for $x=0.6$ along the b axis, which is the highest value at 100 K among various thermoelectric oxides.

-
- [1] I. Terasaki, Y. Sasago and K. Uchinokura: *Phys. Rev. B* **56** (1997) R12685.
- [2] S. Li, R. Funahashi, I. Matsubara, K. Ueno and H. Yamada: *J. Mater. Chem.* **9** (1999) 1659.
- [3] Y. Miyazaki, K. Kudo, M. Akoshima, Y. Ono, Y. Koike and T. Kajitani: *Jpn. J. Appl. Phys.* **39** (2000) L531.
- [4] R. Funahashi and I. Matsubara: *Appl. Phys. Lett.* **79** (2001) 362.
- [5] T. Ito and I. Terasaki: *Jpn. J. Appl. Phys.* **39** (2000) 6658.
- [6] S. Hebert, S. Lambert, D. Pelloquin and A. Maignan: *Phys. Rev.* **B64** (2001) 172101.
- [7] I. Terasaki: *Materials Transactions.* **42** (2001) 951.
- [8] H. Leligny, D. Grebille, O. Pérez, A. -C, Masset, M. Hervieu, C. Michel and B. Raveau: *C. R. Acad. Sci. Paris t.2, IIc* (1999) 409.
- [9] G. A. Wieggers, and A. Meetsma: *J. Alloys Compounds* **178** (1992) 351.
- [10] Y. Matsui, H. Maeda, Y. Tanaka and S. Horiuchi: *Jpn. J. Appl. Phys.* **27** (1988) L372.
- [11] Y. Matsui, A. Maeda, K. Uchinokura and S. Takekawa: *Jpn. J. Appl. Phys.* **29** (1990) L273.
- [12] T. Yamamoto, I. Tsukada, K. Uchinokura, M. Takagi, T. Tsubone, M. Ichihara and K. Kobayashi: *Jpn. J. Appl. Phys.* **39** (2000) L747.
- [13] V. J. Emery and S. A. Kivelson: *Phys. Rev. Lett.* **74** (1995) 3253, and references therein.
- [14] T. Fujii, I. Terasaki, T. Watanabe and A. Matsuda: will be published in *Physica C*; cond-mat0204187.
- [15] P. Kink, D. Jaccard and P. Lejay: *Physica* **B255** (1996) 207.
- [16] I. Terasaki, I. Tsukada and Y. Iguchi: will be published in *Phys. Rev. B*; cond-mat0202089.
- [17] D. J. Shingh: *Phys. Rev. B* **61** (2000) 13397.
- [18] Y. Ando, K. Segawa, S. Komiya and N. Lavrov: cond-mat0108053